Journal of Geophysical Research: Oceans

RESEARCH ARTICLE
10.1029/2017JC013645

Relative Sea Level, Tides, and Extreme Water Levels in Boston Harbor From 1825 to 2018

S. A. Talke[1], A. C. Kemp[2], and J. Woodruff[3]

[1]Department of Civil and Environmental Engineering, Portland State University, Portland, OR, USA, [2]Department of Earth and Ocean Sciences, Tufts University, Medford, MA, USA, [3]Department of Geosciences, University of Massachusetts, Amherst, MA, USA

Key Points:
- Archival research recovered instrumental water-level measurements from Boston (MA) since 1825
- Between 1825 and 2017, relative sea level rose by 0.28 m and accelerated at 0.023 mm/yr^2, while tide range decreased by 5.5% in the 19th century
- Nonstationarity in Boston's flood hazard is driven by relative sea level rise and influenced by trends and nodal variability in astronomic tides

Supporting Information:
- Supporting Information S1
- Data Set S1
- Data Set S2
- Data Set S3
- Data Set S4
- Data Set S5

Correspondence to:
S. A. Talke,
talke@pdx.edu

Citation:
Talke, S. A., Kemp, A. C., & Woodruff, J. (2018). Relative sea level, tides, and extreme water levels in Boston harbor from 1825 to 2018. *Journal of Geophysical Research: Oceans*, *123*. https://doi.org/10.1029/2017JC013645

Received 18 NOV 2017
Accepted 25 APR 2018

Abstract Using newly-discovered archival measurements, we construct an instrumental record of water levels and storm tides in Boston (MA) since 1825. After ascertaining the 19th century datum and correcting for a 0–0.03 m bias in the modern tide-gauge record, we show that local, decadally-averaged relative sea level (RSL) rose by 0.28 ± 0.05 m since 1826, with an acceleration of 0.023 ± 0.009 mm/yr^2. Tide range decreased by 5.5% between 1830 and 1910, due in large part to dredging and filling of Boston Harbor, and trended slightly upward thereafter. An evaluation of storm events since 1825 suggests that trends in flood risk are driven by RSL rise, with a small contribution by tidal trends. Sea-level rise also interacts with the 18.6 year nodal cycle in tide amplitudes to produce decadal fluctuations in hazard. Conditional sampling of the 1825–2018 record shows that storm tides with a 0.01–0.5 annual probability (100 and 2 year events) are 0.1–0.2 m larger during periods with above-average tidal amplitudes. Similarly, the once-in-25 year event during elevated tidal forcing becomes a once-in-100 year event during periods of reduced tides. A plurality of historic flood events—including floods in 1851, 1978, and 2018—occurred near the peak of the tidal nodal cycle. Projections to the year 2100 suggest that decadal fluctuations in tide characteristics will interact with relative sea-level rise to produce a fluctuating hazard over time, with periods of relative stationarity (e.g., the 2020s) bracketed by relatively abrupt increases in flood hazard (the early 2030s).

Plain Language Summary We show that sea-level in Boston (MA) rose by nearly a foot (0.28m) over the past 200 years, with most occurring since 1920. The underlying tide measurements we analyzed were made, in part, by local civil engineers in the 1800s and early 1900s who measured daily high and low tides to help solve design problems and protect infrastructure from flooding. One of those structures, dry-dock number 1 from 1833 at the Charlestown Navy Yard, currently houses the USS Constitution and-if you know where to look-contains a benchmark from 1867 that allows historic measurements to be compared to modern data. The fact that this dry-dock was flooded twice in early 2018 is visceral evidence that sea-level is higher now than it used to be. The old data also shows the interesting-and unexpected–result that some historical extremes were larger in Boston than they would be today because tides were larger. Looking forward, we show that the 18.6 year astronomic cycle in tides also impacts flood risk. During the 2020s, tides will be lower than average, partially mitigating against sea-level rise effects; In the early 2030s, tides will be larger (as in 2018), exacerbating projected sea-level rise effects.

1. Introduction

In January and March of 2018, two extratropical cyclones caused flooding in the Boston (MA) region, and were, respectively, the first and third highest water levels measured (relative to a fixed datum) since modern records began in 1921. Historic relative sea-level rise (RSL; e.g., Kopp, 2013; Sallenger et al., 2012) may have increased the likelihood of record-breaking flooding by pushing hazard curves upward, even if the magnitude of storm tides (the net effect of tidal and meteorological forcing) remained statistically stationary (e.g., Kemp & Horton, 2013). However, both storm events occurred near maxima in the monthly and 18.6 year nodal tidal cycles (Ray & Foster, 2016). At many locations, observations, and modeling suggest that tides and storm tides can evolve through time due to RSL rise, channel deepening, and other factors that alter

system depth (e.g., Arns et al., 2017; Familkhalili & Talke, 2016; Talke et al., 2014; Wang et al., 2018). To put the recent events in Boston in perspective and to determine whether these flood events are statistical anomalies or part of a long-term trend, we use archival research to construct and analyze a nearly 200-year long instrumental record of water-level changes in Boston Harbor.

Instrumental water-level measurements are among the oldest oceanographic records and remain the most accurate method to detail long-term RSL change, evolving tidal regimes, and extreme water levels caused by storm surges (e.g., Talke & Jay, 2013, 2017). Such instrumental records quantify changes in global mean sea level over time and help to establish when modern rates of rise began (e.g., Church & White, 2011). However, analysis of trends on time scales longer than ~100 years is hindered by the scarcity of RSL records from the 19th and early 20th centuries, as well as a spatial and temporal bias in their distribution (Church & White, 2011; Hogarth, 2014). Despite statistical techniques that account for the uneven spatial and temporal distribution of available records (e.g., Dangendorf et al., 2017; Hay et al., 2015; Jevrejeva et al., 2008), establishing global mean sea level trends ultimately relies on the underlying data sets, which makes long (>100 years) instrumental records particularly valuable, especially from outside of Europe (Woodworth et al., 2009). Long RSL records also provide insight into the physical processes (e.g., ocean circulation, plate tectonics, and glacial isostatic adjustment) that drive regional-scale and local-scale trends.

In the western Atlantic Ocean, the longest, currently available instrumental record is from New York Harbor, where the monthly RSL record is ~75% complete since 1856 (National Oceanic and Atmospheric Administration, NOAA, station number 8518750) and additional tidal observations are available since 1844 (Talke et al., 2014). However, at least 6,500 station-years of documented US tide measurements made before ~1970 are not represented in modern databases, of which approximately 25% have been located in paper form (Talke & Jay, 2017). More than 50 records at distinct locations begin in the 19th century, including at least 10 in the Northeastern states (Talke & Jay, 2013, 2017; Figure 1). Tabulations of mean annual water levels from only a few of these historical stations have been used to estimate RSL (Hogarth, 2014; Maul & Martin,1993), and only a few studies (Bromirski et al., 2003; Chant et al., 2018; Familkhalili & Talke, 2016; Talke et al., 2014) have evaluated the underlying high-resolution data to evaluate changes to tides or extremes, or assess data quality.

We detail the recovery, datum reconstruction, digitization, quality assurance, and analysis of 50 years of pre-1920 tide records from Boston Harbor that we found in documentary archives. The tabulations of daily water-level data, combined with archival notes, correspondence, and reports, enable us to assess data quality, document datum shifts, and estimate biases and uncertainty associated with sampling errors and vertical control in both the historic and modern (post-1921) data. When combined with available NOAA measurements since 1921 (station number 8443970), these records span the period 1825–2018 to form the longest known water-level record outside of Northwest Europe (Figure 1b; Talke & Jay, 2017). We use the newly recovered measurements to: (1) describe the patterns and causes of RSL trends in Boston since 1825, and assess the onset of modern RSL rise; (2) constrain how and why tide range in Boston evolved through time; and (3) investigate extreme events and determine whether factors besides RSL rise in Boston are producing nonstationarity in flood risk.

2. Methods

2.1. Setting

The water-level measurements we consider are primarily from the inner part of Boston Harbor (MA) and were primarily made at gauges located within ~3 km of one another (Figure 1). As shown later, the relatively close spacing means that there is no noticeable shift in tidal properties between different locations, or measureable bias in storm heights. However, the geography and bathymetry of Boston Harbor has altered greatly over the past two centuries and is a possible source of nonstationarity in the gauge records. To show how the surface area of the bay changed over time, we combined the presettlement boundaries maps from Seasholes (2003) with early and mid-19th century bathymetric maps (e.g., from https://www.nauticalcharts.noaa.gov/csdl/coastalmaps.html) to estimate the 1830 land/ocean boundary. Additionally, we used the Coast and Geodetic Survey map from 1915 (NOAA map 337-8-1915) to estimate land boundaries at the start of the modern NOAA record.

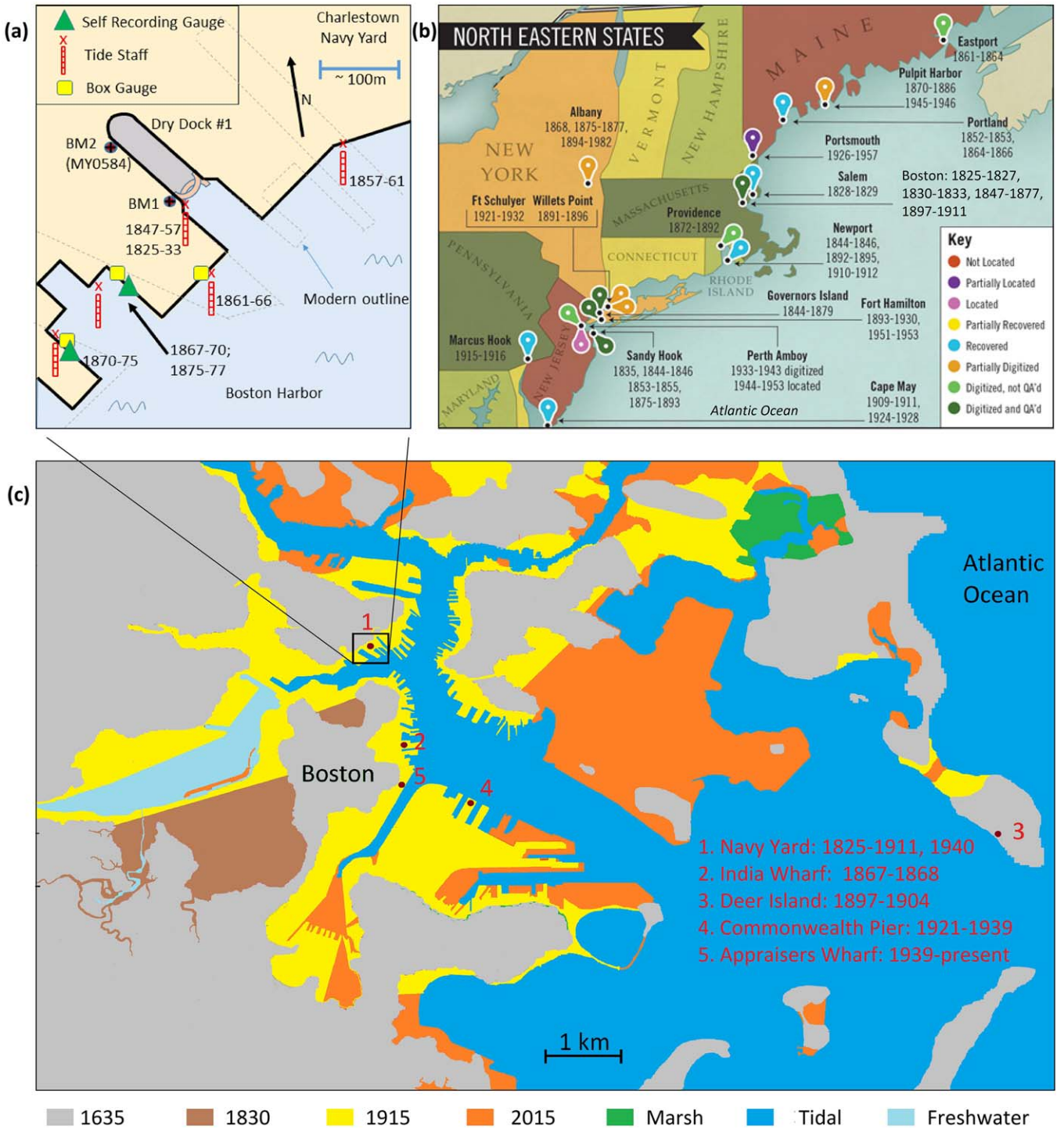

Figure 1. (a) Close-up of tide-gauge locations at dry dock #1 at Charlestown Navy Yard, adapted from Freeman (1903), Schureman (1928), and archival letters. (b) Overview of known locations of historic data sets not represented in modern databases along the US East Coast, adapted from Talke and Jay (2017), and (c) An overview of the five gage locations within Boston Harbor used within this study, plus an approximation of land reclaimed over time. Land reclamation within Boston City Limits is well described by Seasholes (2003); these records were augmented by review of historic maps available from NOAA. The amount of land reclaimed is probably more extensive than shown here, since some ambiguity about historical marsh boundaries exists. Note that the Charles River was cutoff from tidal action and turned into a freshwater basin in 1910.

Approximately 21 km^2 of land reclamation occurred between 1800 and 1975 (Seasholes, 2003), with the majority occurring between the advent of railways (~1830) and 1915 (Figure 1). Demographic factors, combined with a plan to scour the shipping channel to improve access for large vessels into and out of the harbor, led to large-scale reclamation projects in the mid and late 19th centuries in South Boston and the Charles River (Seasholes, 2003; see also Freeman, 1903). The Charles River Dam (completed 1910) cutoff tidal action to the Charles River, and airport development (1915–1975) further reduced the surface area of the harbor. Dredging began in the early 1900s, and by 1915 the harbor was deepened from its original controlling depth of ~8 m to 10.7 m. Between 1930 and the 1950s, various regions of the harbor and approaches were further dredged to 12.2 m. Anthropogenic changes continue, and, for example, the shipping channel was recently authorized to be widened to 275 m and deepened to 15.5 m (United States Congress, 2014).

2.2. Archival Research: History of Tide Measurements in Boston Harbor

The history of water-level measurements made in Boston Harbor is longer than the continuous 1921–2018 record available from the NOAA-operated tide gauge (station number 8443790). Research in libraries, archives, and historical reports (see supporting information) indicates that private citizens may have taken tide measurements or tabulated high-water marks by the early 1800s. Records available at Harvard University show that Loammi Baldwin Jr., a well-known civil engineer, was commissioned in the 1820s by the US Federal Government to construct Dry Dock 1 at the Charlestown Navy Yard. To design its dimensions and constrain its vertical placement, Baldwin made 422 days of daytime tide measurements between December 1825 and July 1827. An additional 26 months of measurements were made during construction of the dry dock from 1830 to 1833. The US Coast Survey made nearly continuous measurements at the same location from 1847 to 1877, and the US Navy measured tides from 1902 to at least 1911 (Schureman, 1928). These measurements, and other shorter local time series, have essentially remained stored in boxes for more than a century (e.g., Talke & Jay, 2013).

We found, recovered, and digitized a total of 50 years of high/low and hourly water-level measurements (Figure 1a). Approximately 42 months of data spanning the years 1825–1833 (the Baldwin data) were recovered from libraries at the Massachusetts Institute of Technology (MIT) and Harvard University, along with an additional 7 years of data from 1897 to 1904 and a 1 year record from 1867 to 1868. We also found 40 years of records between 1847 and 1911 at the US National Archives (for location and time, see Figure 1 and supporting information). Details, including selected images of data, letters, and other records, are included in the supporting information.

The modern Boston tide gauge (NOAA station number 8443970) was installed in 1921 by the US Coast and Geodetic Survey at Commonwealth Pier 5, ~3 km from the historical Charlestown Navy Yard location (Figure 1). In January 1939, the gauge was moved to its current location at the Appraisers Wharf (see Figure 1). We also recovered and digitized hourly measurements made by the US Coast and Geodetic Survey at the Charlestown Navy Yard (NOAA station number 8443838) from February to October 1940. These measurements, along with daily staff/gauge comparisons and leveling information for the 8443970 and 8443838 gauges, were downloaded from the EV2 database at the National Centers for Environmental Information (https://www.ncdc.noaa.gov/EdadsV2) and are used to help reduce records since 1825 to a common datum (see below).

2.3. Storm Events—Data Recovery and Analysis

The newly recovered data contain quantitative measurements of pre-1920 extreme water levels, including notable events in 1832, 1851, and 1909. From archival notes and historical documents, we also estimated additional high-water marks from storms events between 1723 and 1919 (e.g., Bearss, 1984; Freeman 1903, 1904; Ludlam, 1963; Perley, 1891; Public Works Department (PWD), 1922; Smith, 1917; United States House of Representatives (USHR), 1830; Wood, 1978; see supporting information S.4 for a full description). During the data gap from 1834 to 1846, the only storms of note occurred in 1839; similarly, newspaper records from 1877 to 1896 suggest that the only significant high-water event occurred in 1885. The 1897–1920 period is well documented (Freeman, 1903; PWD, 1922). Hence, combined with the 50 years of recovered instrumental data, we propose that all significant storm tides above ~2.3 m from 1825 to 1920 are likely accounted for. Tabulations of monthly extremes for 1921–2018 (NOAA station 8443970) are used to determine modern high-water marks.

The probability of a large storm tide is evaluated using the Generalized Pareto distribution (GPD; see e.g., Kotz & Nadarajah, 2000), a peak-over-threshold approach that allows the use of several large events in a year (as occurred, e.g., in 1851, 1898, and 2018). The peak-over-threshold approach can be used as long as all events over a threshold are characterized (even if those below the threshold are not). The shape and scale parameters are found using a maximum likelihood estimation method. Following standard procedure, we increased the threshold until the shape and scale parameter in the GPD distribution converged. Hence, experimentation showed that a storm-tide threshold of 2.4 m adequately modeled the tail of the distribution, while retaining sufficient data for analysis. A total of 83 known storm tides from 1825 to 2018 exceeded this limit (see supporting information), evenly distributed before 1921 (43 events) and after 1921 (40 events). Event independence was ensured by requiring at least a 5 day offset between successive events. To ground-truth our approach, we also compare GPD results to an unbiased return period from order-ranked data (see e.g., Makkonen, 2006), Additionally, we compare GPD results to return-period estimates calculated by NOAA using annual maxima data since 1921 and the Generalized Extreme Value (GEV) approach (see Kotz & Nadarajah, 2000).

The contribution of tides to storm high-water marks is estimated using the harmonic analysis program *t-tide* (e.g., Leffler & Jay, 2009; Pawlowicz et al., 2002), based on a 369 day analysis that includes 68 constituents and enables the semiannual (SSA) and annual (SA) constituents to be estimated. Predictions are made with the default nodal corrections (Pawlowicz et al., 2002), using constituents that have a signal-to-noise ratio greater than two. Tidal datums such as the Highest Astronomical Tide (HAT) and Mean Higher High Water (MHHW) are obtained from NOAA (station number 8443970). Following NOAA definitions, the Mean Tide Range is calculated as the difference between Mean High Water and Mean Low Water, while the Mean Tide Level is the average of Mean Low Water and Mean High Water. We define a storm tide to be the measured water level minus the annual mean sea level for that year. In turn, we define skew surge to be the difference between the maximum measured storm tide and the predicted astronomical tide (e.g., Williams et al., 2016). The datum for *Moderate flooding* and *Major Flooding* was obtained from the US National Weather Service.

2.4. Benchmark and Datum History

The datum and benchmarks used in the 1847–1877 and 1902–1911 times series (see Figure 1 for locations) are extensively discussed in Freeman (1903) and Schureman (1928). To assess the 1825–1833 datum, improve the interpretation of the post-1847 Charlestown Navy Yard datum, and correct the modern station datum for a slight bias, we consulted additional letters and other ancillary material found in archives (see below and supplement). The key to defining the 1825–1833 datum was to determine the definition of the tidal datum used by Laommi Baldwin Jr., and its relationship to the design height of the dry dock coping (i.e., the top surface). In the final design, as also confirmed by letters and maps after construction (Freeman 1903; USHR, 1830), the coping was placed 5 feet (1.5 m) above *Ordinary High Water*, which Baldwin Jr. explicitly calculated to be the tide level that was exceeded by 2/3rds of the tabulated high waters (see letters in supporting information S.6).

All subsequent tide measurements at the Charlestown Navy Yard between 1830 and 1940 used the coping of the dry dock as a vertical reference point (e.g., Baldwin, 1864; Freeman, 1903; Schureman, 1928). Two benchmarks were monumented into the dry dock, as shown in Figure 1, and the second, from 1867, still exists. However, as extensively documented by Freeman (1903), the action of frost heave gradually lifted the coping at BM 1 by $\sim$0.47 ft (0.14 m) between 1830 and 1900. Fortunately, repeated leveling indicates that BM 2 remained stable in the 19th and 20th centuries, which enables a reliable tie to the modern datum (Freeman, 1903; Schureman, 1928; NOAA leveling records thru 1944, and National Geodetic Survey Records; see supporting information S.2 and S.6, and Table S.2.1).

Using extant survey information, we reduced post-1867 data to the reference frame of the stable BM 2. In addition, we applied a time-variable correction to the pre-1867 time series, based on an estimate of the frost-heave rate from leveling surveys (see supporting information S.2). After applying our datum interpretation, our estimates of the 1847–1877 datum lie between those of Schureman (1928) and Freeman (1903). While the Freeman/Schureman interpretations incorrectly assumed an unstable BM 2 (see supporting information for details; also Hogarth, 2014), they are useful for defining a cone of datum uncertainty of order $\pm$0.05–0.06 m for data prior to 1857, $\pm$0.04 m for 1857–1860, $\pm$0.03 m for 1861–1866, and $\pm$0.02 m for

Table 1
Estimated Accuracy (Precision Plus Datum Bias) in an Annually-Averaged Sea-Level Measurement Based on the Historic New York and Boston Tide-Gauge Measurements

Time period	Estimated accuracy of Boston measurement	Time period	Estimated accuracy of New York measurement
1825–1833	±0.05 m		
1847–1856	±0.06 m		
1857–1860	±0.05 m	1856–1861	±0.06 m
1861–1868	±0.04 m	1862–1869	±0.04 m
1869–1876	±0.03 m	1870–1879	±0.03 m
1897–1904 (Deer Island)	±0.06 m		
1902–1911	±0.04 m	1893–1926	±0.02 m
1921–1939	±0.03 m (before corrections described in supporting information S.2.2) ±0.01 m (after correction)	1927–present	±0.01 m
1939–1960	±0.02 m (before corrections described in supporting information S.2.2) ±0.01 m (after correction)		

Note. We have combined measurement uncertainty and bias under the assumption that they are uncorrelated. See supporting information for details.

1867–1876. These combine with measurement uncertainty (below) to produce a composite error estimate (Table 1). Available evidence suggests our interpretation reduced bias and that accuracy is better than suggested above. For example, comparisons of annual RSL at the Charlestown Navy Yard and at the India Wharf from 1867 to 1868 agree to within 2 mm. Further, our instrumentally based estimate of maximum water level during the 1851 Minot's Ledge storm (4.74 m above the Boston Base datum) agrees well with an estimate based on the average of 12 high-water marks that were surveyed shortly after the storm (4.76 m above Boston Base; PWD, 1922). Finally, RSL measured relative to the original coping datum for 1826–1827 and 1830–1832 is consistent with mid 19th-century RSL (see results) and thus provides an important plausibility check. The datum for water levels measured at the India Wharf (1867–1868), Deer Island (1897–1904), and the Charlestown Navy Yard (1902–1911) is obtained from Freeman (1903). When these measurements are included, the RSL record for Boston Harbor between 1825 and 2017 becomes ~75% complete (146 years out of 193 represented). See results and supporting information for more details.

2.5. Quality Assurance and Bias Correction

Several direct and indirect methods are used to estimate measurement precision. Water-level observations from 1867 to 1876 and 1921 to 1983 included manual, approximately daily comparisons of the vertical difference between readings of the tide-staff and the self-registering tide gauge. For 1867–1876 data, we estimate a precision of ±0.02 m in estimates of annual mean sea level, based on calculations of the mean staff/gauge difference and its standard deviation. After 1921, the precision is approximately ±0.01 m. A similar difference in pre-1920 and post-1920 precision is found by comparing the difference between minimum and maximum RSL in each decade. Under the assumption that the larger decade-by-decade variability in pre-1920 data is an artifact of measurement (and datum) error rather than a physically caused signal, we estimate an uncertainty of ±0.02 m for RSL during 1826–1832 and 1847–1866, and a slightly larger uncertainty of ±0.03 m for 1897–1911 (see supporting information S.2.5).

Additional tests were made to assess historic data quality. Data were detided using harmonic analysis (e.g., Leffler & Jay, 2009) and the residual inspected for unexplained datum shifts or other anomalies. Clock errors, which are often a proxy for stilling well siltation and other problems (Zaron & Jay, 2014), were tested using a method based on Agnew (1986) and Hudson et al. (2017). A limited number of problematic data were found (e.g., February 1865; August 1867; a few months in 1873 and 1874; June 1951; and a few months in 1971–1974). These infrequent problem measurements, some of which are confirmed by archival notes, have a negligible influence on long-term patterns. Nonetheless, the data were removed from annual estimates for consistency (see supporting information for details).

Small bias corrections of <0.02 m were made to account for under-sampling in historic data and the small bias introduced by sampling only daytime high and low tides in the 1820s (supporting information S.3.3). A mean offset of 0.037 m was used to convert mean tide level to mean sea level (a small nodal correction was also applied). To minimize uncertainty, we report annual statistics only for years with at least four months of measurements. Simultaneous mean tide level estimates between 1902 and 1904 suggest that Deer Island mean tide level estimates were biased 0.04 ± 0.03 m high relative to the Charlestown Navy Yard measurements. We apply this mean correction to 1897–1901 Deer Island data, but recognize that a datum uncertainty of perhaps ±0.03 m attends these measurements. Overall, the 1897–1911 data have greater uncertainty than earlier and later measurements.

2.6. Modern Datum Bias

Leveling records suggest that the Commonwealth Pier data (1921–1939) and the Appraisers Pier data (1939–present) from the Boston gauge (8443970) should be corrected for slight datum instability. Between 1921 and 1939, leveling records show that the station datum sank by 0.027 m ± 0.003 m relative to a fixed local datum, due both to a lowering of the staff zero and subsidence in the primary benchmark. Applying the correction results in a slight reduction in the total RSL rise since 1921 (see section 3). Available daily staff/gauge comparisons in the EV2 database from 1939 to 1984 show that the station datum was occasionally adjusted in postprocessing to retain a constant vertical offset with the then-primary benchmark (BM 13). However, BM 13 was later considered unstable, and bias corrections were applied by NOAA back to 1939 to put measurements into the reference frame of benchmark K 12, the current primary benchmark. Nonetheless, careful evaluation suggests that an additional bias correction of 0.004–0.011 m is still required for data between 1939 and 1974 (see supporting information S.2 for details; the correction is also attached as supporting information).

2.7. Datum Tie Between Historical and Modern Data

After applying the corrections described above to modern data, we obtained the offset between pre-1920 data (referenced to BM 2) and the modern station datum by four independent methods:

1. Applying the results of the leveling survey between BM 2 and gauge 8443970 made in 1923 (see Schureman, 1928), after correcting for the subsidence in the station datum between 1923 and 1939.
2. Connecting BM 2 to the Boston Base datum via Freeman (1903), and applying known offsets between the Boston Base datum and the North American Vertical Datum of 1988 (NAVD88).
3. Comparing sea-level measurements in 1940 at the Boston and Charlestown Navy Yard sites.
4. Using the tabulated NAVD88 heights of BM 2 and the Boston station datum (NOAA 8443790).

These four-independent ties suggest that BM 2 is/was 5.40 m ± 0.01 m (17.71 ft ± 0.03 ft) above the present-day station datum (defined to be 22.496 ft below K 12; e.g. supporting information Figure S.2.11), and verify that correcting modern data for its slight bias in the early to mid 20th century improves the tie. The relatively small variability between different connections also suggests that benchmarks BM 2 (primary benchmark before 1920) and K 12 (primary benchmark since 1939) have approximately equal subsidence rates, and are likely stable relative to the local Boston Base datum.

2.8. New York Sea Level

Using the tide records from New York harbor described in Talke et al. (2014), we reevaluated the 1856–1861 portion of the New York monthly data set (NOAA station 8518750) and made a preliminary estimate of datum uncertainty from 1856 to 1927 (Table 1). Specifically, we infilled a missing year of data (1861) and recomputed monthly averages for 1856–1860 using manual observations of daily high/low measurements that were made on a box gauge. Our recomputation changes the standard deviation of monthly data from 1856 to 1860 from 0.038 m (NOAA data) to a more realistic 0.089 m, which is statistically more similar to 1862–1878 monthly data ($\sigma = 0.086$ m). The corrected data also reproduces a typical seasonal cycle (see supporting information). The changes increase the 1856–1861 average by 0.015 m, partially because RSL in 1861 was higher than in previous years (also in Boston data). We estimate that the accuracy in the New York RSL record is ±0.06m from 1856 to 1861, ±0.04 m from 1862 to 1869, ±0.03 m between 1870 and 1879, and ±0.02 m from 1893 to 1927 (Table 1). Additional details about the reevaluated New York records are available in supporting information S.2.6.

2.9. Sea Level Analysis

A primary reason to recover additional archival sea-level data is to corroborate existing records, improve composite estimates of long-term trends and variability (e.g., Hogarth, 2014), evaluate uncertainty, and investigate whether regional-scale RSL differences among stations are due to plausible physical processes and/or uncertainty in records. We therefore compare long-term trends and the observed interannual variability in the New York City RSL against the extended Boston RSL record, after correcting for the estimated contribution from vertical land motion produced primarily by glacio-isostatic adjustment (GIA). GIA, which is the response of the Earth to the loading and unloading of continental ice during glacial and interglacial periods, causes recent RSL rise in Boston and New York City through subsidence and reorganization of the geoid, and is generally considered linear over the 100–200 year scale under consideration here (Davis & Mitrovica, 1996; Peltier, 2004). Earth-ice model predictions, permanent Global Positioning Satellite measurements (Karegar et al., 2016), late Holocene RSL reconstructions (Engelhart & Horton, 2012), and statistical analysis of tide-gauge records (Kopp, 2013; Zervas et al., 2013) suggest that GIA contributed approximately 0.5–0.8 mm/yr to RSL trends in Boston Harbor, with a confidence of $\pm$0.2–0.3 mm/yr. Estimates for New York City typically fall within the range of 1.2 $\pm$ 0.6 mm/yr (e.g., Zervas et al., 2013). When the Karegar et al. (2016) and Kopp (2013) estimates for Boston and New York, respectively, are used, the estimated difference in GIA between the two locations is 0.6 $\pm$ 0.45 mm/yr. A recent analysis by Piecuch et al. (personal communication, 2018) that incorporated tide-gauge records, GPS data, and GIA models in a probabilistic framework estimated that vertical land motion contributed $\sim$0.7 $\pm$ 0.3 mm/yr (median $\pm$ 1 standard deviation) more to RSL rise in New York City than it did in Boston (C. Piecuch, Personal Communication, 2018). Here we correct for vertical land motion using the Piecuch et al. (personal communication, 2018) values of 0.5 $\pm$ 0.6 mm/yr for Boston and 1.2 $\pm$ 0.5 mm/yr for New York. This enables comparison of historic RSL changes from processes other than GIA.

A common method of statistically assessing a change in the rate of RSL rise over time is to estimate its "acceleration," defined by convention to be twice the coefficient of the squared term in a parabola that is fit to RSL data (e.g., Church & White, 2011). Acceleration in RSL, because it is unaffected by uncertainty in the linear GIA correction, provides an alternate methodology for comparing the Boston and New York records. Global surveys suggest an acceleration of 0.006 to 0.018 mm yr^{-2} since 1900 (e.g., Church & White, 2011; Dangendorf et al., 2017; Hay et al., 2015; Hogarth, 2014; Jevrejeva et al., 2008; Woodworth et al., 2009), indicating that linear trends over the period are increasing. Because acceleration is a second-order term in a quadratic fit, it depends on both the magnitude and slope of the underlying data at the beginning and end of the record, and is therefore subject to more uncertainty than linear trend estimates. For New York and Boston, therefore, we evaluate the effect that offsets in (GIA-corrected) sea level and differences in slope may have on the calculated acceleration. Moreover, we also investigate the effect of record length by calculating acceleration with a sliding start date, while keeping the end-date fixed at 2017 (see e.g., Rahmstorf & Vermeer, 2011). By incrementing forward in time (e.g., calculating acceleration for the period 1826–2017, 1827–2017, 1828–2017, . . ., 1970–2017), we test whether the statistics are stable and unaffected by small differences in record length, or whether there is evidence of nonstationarity or change in behavior. An errors-in-variables change point analysis (e.g., Kemp et al., 2013) is also applied to estimate the start of modern rates of rise in Boston RSL.

3. Results and Discussion

3.1. Relative Sea Level (RSL)

Annually averaged water-level data show that RSL in Boston rose by $\sim$0.28 $\pm$ 0.05 m over the 1825–2017 period (Figure 2), with an approximately 0.26 m rise occurring between the 1920s and the decade ending in 2017. RSL changed little during the 19th century, with year-to-year and decadal variability outweighing a slight, statistically insignificant downward trend between 1825 and 1876 (Figure 2a). In the early 20th century, annual RSL began to rise, though only after about 1940 did RSL consistently exceed the bounds of 19th century variability (Figure 2a). Our datum correction to early and mid-20th century data (section 2.6) slightly decreased the RSL rise apparent in the 1921–2017 NOAA record, from 2.8 mm/yr (e.g., Ray & Foster, 2016) to 2.6 mm/yr. Application of errors-in-variables change point analysis (e.g., Kemp et al., 2013) to the annual RSL record indicates that a statistically-significant increase in the rate of RSL rise occurred between 1919 and 1932 (95% credible interval; Figure 2a).

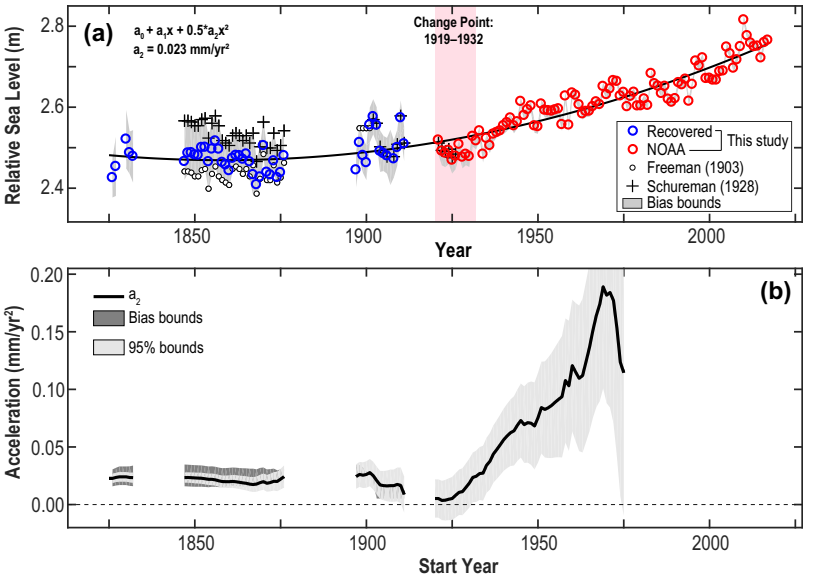

Figure 2. (a) Relative Sea Level in Boston from 1825 to 2016, based on this study's datum interpretation. Data plotted relative to station datum of NOAA gauge 8443970. RSL using the Freeman (1903) and Schureman (1928) datum interpretations are also shown (F1903 and S1928, respectively). (b) Acceleration coefficient a_2 in a parabolic fit using a sliding start date. Bias bounds obtained by using the F1930 and S1928 datum scenarios. The 95% confidence intervals obtained from the least squares fit. The plot is discontinued when a_2 becomes statistically insignificant in the 1970s.

We estimate an average acceleration of 0.023 $\pm$ 0.009 mm/yr^2 (95% confidence interval) from 1826 to 2017 (Figure 2a). When the analysis start date is varied in increments of 1 year from 1826 to 1900 (see section 2.9), we find that acceleration estimates are relatively stable within the range of 0.017–0.026 mm/yr^2 (Figure 2b). These rates are consistent with an analysis of European data, which showed an acceleration of 0.02 mm/yr^2 since the early 1800s (Jevrejeva et al., 2014). Similarly, our estimated acceleration from 1900 to 2017, 0.026 $\pm$ 0.012 mm/yr^2, is consistent with recent analyses of global tide-gauge compilations and satellite altimetry data, which indicate an acceleration of global mean sea level rise of 0.017–0.018 mm/yr^2 since

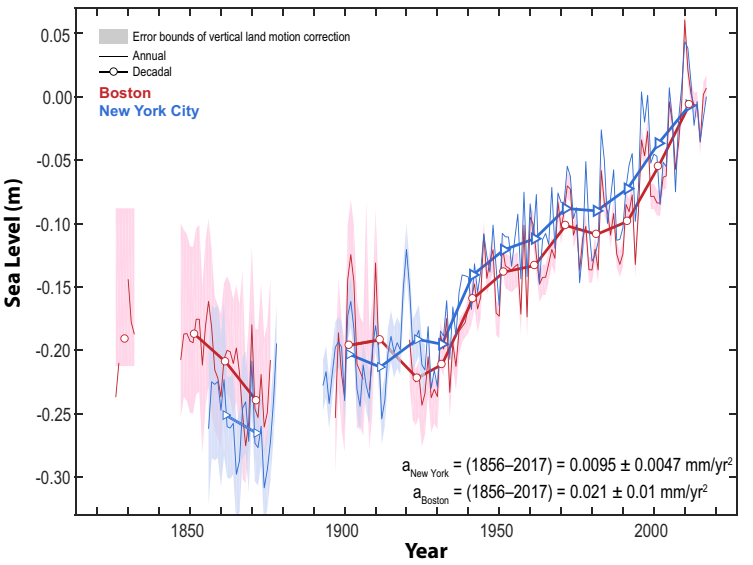

Figure 3. Boston and New York Sea Level after applying a vertical land motion correction to each record relative to the 2008–2017 average (see section 2.9). Thick red and blue lines with squares and triangles denote the Boston and New York decadal average, respectively, while the thin red and blue lines denote annual fluctuations. The overlapping error bounds of the vertical land motion correction are shown by fill around the annual mean.

the late 19th/early 20th century (e.g., Dangendorf et al., 2017; Hay et al., 2015). Similar to patterns found in global data sets (e.g., Rahmstorf & Vermeer, 2011), acceleration estimates decrease for start dates from 1900 to 1920 (Figure 2b), become statistically insignificant between 1921 and 1931, and then transition to much larger rates of up to 0.1–0.2 mm/yr^2 for start dates between 1950 and 1970. For start dates after 1970, the statistical analysis becomes increasingly uncertain due to the shortness of record (c.f. Haigh et al., 2014; Rahmstorf & Vermeer, 2011).

After removing the contribution to RSL from vertical land motion (see section 2.9), sea-level trends since the mid-1800s in Boston and New York City are similar (Figure 3). Both records show little change prior to the early 20th century, after which notable sea-level rise occurred. The observed rise in decadally-averaged sea level between 1901 and 2000 was 0.13 m in Boston and 0.16 m in New York City, which is similar to estimates of global mean sea level rise (0.14–0.19 m) over the same period (e.g., Church & White, 2011; Dangendorf et al., 2017; Hay et al., 2015; Jevrejeva et al., 2014). Similar order-of magnitude differences in annual sea-level between Boston and New York City are observed throughout the 1856–2017 period of data overlap, and are well within the uncertainty bounds of the RSL data at each station (see Figure 2a and Table 1) and the error bounds of the vertical land motion correction (Figure 3). The average offset from 1856 to 1876 (the period of 19th century overlap) is 0.037 m; when this offset is removed, the difference in acceleration rate shown in Figure 3 is halved. The larger acceleration in Boston is also caused by an apparent increase in the rate of sea-level rise in Boston since ~1990, relative to New York, which Davis and Vinogradova (2017) attributed primarily to dynamical processes in the ocean (see convergence post-1990 in Figure 3). When the rise in Boston since 1990 is held constant to New York rates, we find a further reduction in the estimated 1856–2017 acceleration at Boston of 0.003 mm/yr^2. Thus, estimates of acceleration are sensitive to any slight offset or difference in trends found at the beginning or end of the data set, whether caused by measurement uncertainty (Table 1), or dynamical processes such as temporal changes in the spatial variations in wind stress, the inverted barometer effect, water temperature, gravitational fingerprinting, or other physical processes (Frederikse et al., 2017; Goddard et al., 2015; Hay et al., 2015; Landerer et al., 2007; Piecuch & Ponte, 2015).

3.2. Tides

Archival tide measurements suggest that the nodally-corrected, mean tidal range in the inner Boston Harbor decreased by 2.03 mm/yr in the 19th century, from ~3.05 m in 1830 to ~2.89 m in 1910, a reduction of ~5.5% (Figure 4a). After 1930, tidal range increased at 0.19 mm/yr. Similarly, mean high water decreased at a rate of ~1 mm/yr between 1830 and 1910. Both local and regional processes are likely causes of observed patterns. Tides in the Gulf of Maine are sensitive both to RSL variations and possibly alterations in

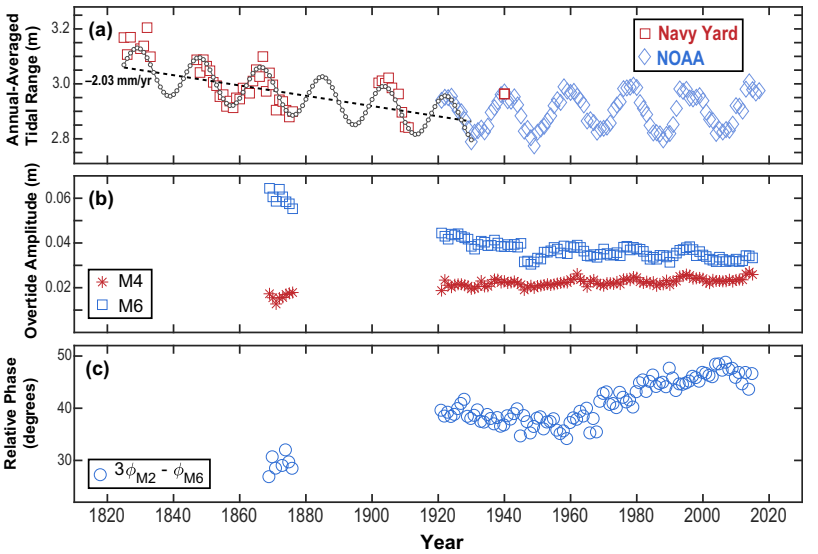

Figure 4. Temporal changes in (a) annually averaged tide range, (b) overtide amplitudes, and (c) the relative phase for M6 in Boston Harbor.

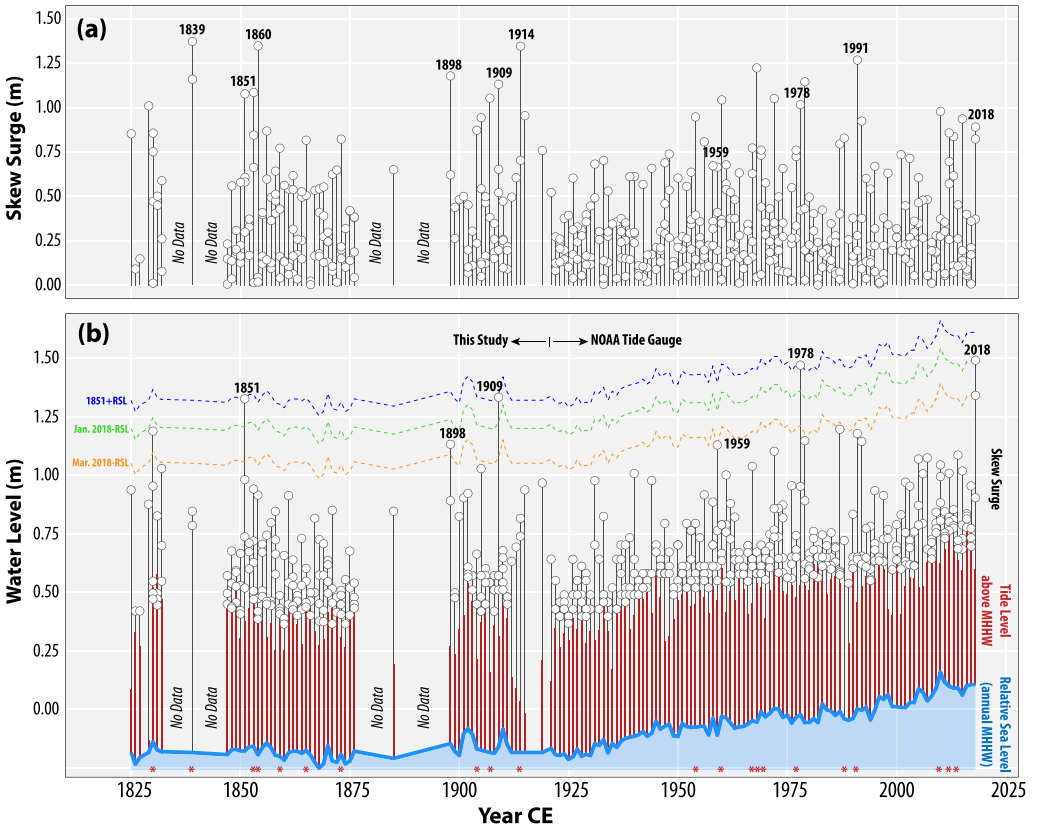

Figure 5. (a) The skew surge associated with the top 500 measured water-level events and (b) the top 500 water levels relative to the MHHW datum for the 1983–2001 epoch, defined to be 4.205 m over station datum and 1.45 m over NAVD-88. Sea level rise is shown by the increase in mean higher high water. The total still water level of the event (open circle) is the sum of sea level rise (blue), the predicted tide (red bar), and the skew surge (black line). The dashed lines show the height of the 1851, January 2018, and March 2018 events as sea level rises (under the assumption of the same predicted tide and measured skew surge).

stratification, due to the well-documented resonance of the M2 constituent (e.g., Ray, 2006; Ray & Foster, 2016). Tide constituents may also be shifting within the northwestern Atlantic (Müller, 2011; Woodworth, 2010); for example, the M2 tide at Sandy Hook, NJ decreased by ~0.027 m ± 0.01 m between the 1870s and 1930s, and increased by 0.02 m thereafter (Talke et al., 2014). Similarly, a secular decrease in the S2 constituent occurred during the 20th century at many East coast locations (Ray, 2006; Woodworth, 2010).

Simultaneously, local perturbations to tides may be caused by the systematic, extreme alteration in the bathymetry and surface area of the inner Boston Harbor and its approaches (Figure 1; Seasholes, 2003). Analysis of overtide constituents (Figures 4b and 4c), which are produced by nonlinear (frictional) interactions in shallow water, strongly suggests that altered tide properties are influenced by the loss of more than 20 km^2 of shallow water habitat (Figure 1) and the deepened shipping channel. All other constituents remaining equal, the collapse in the M6 overtide (Figure 5b) since the 1870s produces a 0.04 m (2.5%) decrease in tidal range, approximately 0.03 m due to its shifting amplitude and 0.01 m due to a change in its relative phase with M2 (defined as $3\varphi_{M_2} - \varphi_{M6}$). These changes are partially offset by changes to M2, which decreased by ~0.015 ± 0.005 m between the 1870s and 1920s, but increased by nearly 0.03 m from the 1920s to the present (see also Ray & Foster, 2016). Tidal range increased less than M2 since 1921, likely due to changes to overtide amplitudes and phases. Between 1825 and 1867, the lack of time resolution in high/low data precludes the separation of the M2 constituent and the M6 overtide by harmonic analysis (e.g., Foreman, 1977). Nonetheless, reducing the sum of the constituent amplitudes of M2 and M6 by 0.06–0.08 m between 1830 and 1870 would explain the observed decrease in tide range.

We hypothesize that several local physical processes help explain the secular change in tidal range. First, tides are amplified by approximately 10% in the ~15 km between the harbor entrance (e.g., Boston Light)

and the Boston Inner Harbor (Table 30 in Schureman, 1928). Hence, the changing length, width, and depth of the inner harbor, as well as coastline hardening, may affect the reflection of the tide wave, and/or the convergence properties, leading to an altered tidal range. Moreover, increasing the average system depth H (e.g., by dredging) has a similar dynamic effect as decreasing the drag coefficient C_d (e.g., Friedrichs & Aubrey, 1994; Chernetsky et al., 2010). In a system such as Boston, with little river flow, one might expect that production of the M6 overtide would be most affected by bathymetric change. Specifically, analytical models of tides often expand and linearize the friction coefficient $\frac{C_d U|U|}{H}$ into a cubic function of velocity U (e.g., Dronkers, 1964; Godin, 1991; Kulkuka & Jay, 2003). For a system with low river discharge such as Boston, U is dominated by tides, which results in the production of the M6 overtide (Godin, 1991; Parker, 1991). Therefore, the collapse of the M6 overtide in Boston Harbor likely reflects the greater average depth of the system caused both by channel deepening and by the significant loss of subtidal and intertidal habitat (Figure 1). Interestingly, the M4 overtide slightly increased over time (Figure 5b), possibly indicating an increase in the (small) tidally averaged flow (e.g., river discharge or the return flow caused by tidal Stokes drift—see, e.g., Moftakhari et al., 2016) but also potentially caused by a decrease in damping of the overtide produced on the continental shelf (e.g., as occurs in the Ems Estuary; see Chernetsky et al., 2010). The divergence in the M4 and M6 overtide trends is an interesting challenge for a future numerical or analytical model to reproduce and explain.

3.3. Storm Tides

In January 2018, an extratropical cyclone caused water levels to reach ~2.93 m above the NAVD-88 datum, which is the highest level ever recorded by the NOAA tide gauge. Two months later, a second extratropical cyclone produced the third highest water level since 1921, slightly lower than water levels during the well-known 1978 blizzard, which was previously the storm of record for Boston. To properly frame the factors producing these extreme water levels and to establish how unusual (or indeed common), the 2018 events are over century time scales, we next analyze historic extreme water-level events.

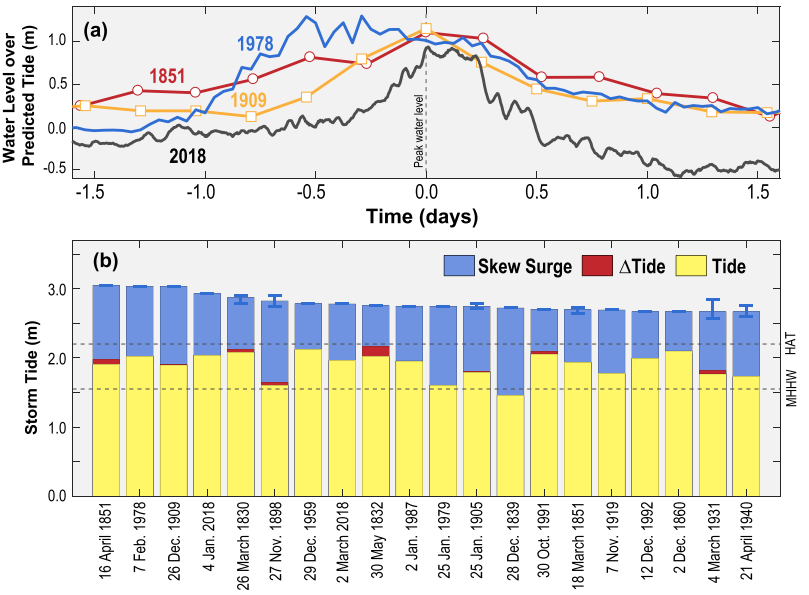

Figure 6. (a) The super-elevation of water level over predicted tides for the four largest events since 1825 and (b) the top 20 storm tides since 1825. In Figure 6a, the graphs are centered such that the peak water level over a datum occurred at $t = 0$. In Figure 6b, the storm tide, defined as the difference between the peak water level and annual mean sea level, is broken into three components: (i) the predicted tide using a harmonic analysis of hourly data from station 8443970 (yellow), (ii) the skew surge, defined as the storm tide minus the predicted high water (blue), and (iii) the difference between historical and modern predictions, ΔTide (red). The modern values for Mean Higher High Water (MHHW) and Highest Astronomical Tide (HAT) relative to MSL are also displayed. Pre-1920 tides are predicted using harmonic analysis of hourly data from 1874; M2 is adjusted for each year such that predicted tide range reproduces the secular change in tide range between 1830 and 1910 (Figure 4). In Figure 6a, the 1851 and 1909 events depict skew surge, while the 1978 and 2018 event are surge (measured minus predicted water level). Uncertainties for ungauged events, which are discussed in supporting information S.4, are depicted with error bars.

Records show that many significant storm events occurred before the start of the modern record in 1921, with particularly large flooding occurring in 1723, 1786, 1830, 1851, 1898, and 1909 (Figures 5b and 6; see supporting information for pre-1825). Of the 100 largest storm tides that we identified since 1825, 87 were extratropical cyclones that occurred between 1 November and 30 April. The occurrence of two large storm tides in a year, as in 2018, is rare but occasionally occurs (e.g., 1851 and 1898). Only one hurricane-influenced event, the hybrid "Perfect Storm" (1991), makes the top 20 list (Figure 6). The Expedition Hurricane (3 November 1861; 2.64 m storm tide) and hurricane Carol (30 August 1954; 2.42 m storm tide) are the only other confirmed tropical storms in the top 100. Large hurricane storm tides may have occurred in 1635, 1743, and 1770 (see Ludlam, 1963), but accounts are fragmentary, qualitative, and difficult to relate to a datum (see supporting information S.4). In conclusion, the flood hazard for return periods less than 300 years (the length of available records) is driven by extratropical cyclones. This contrasts with locations further south such as New York City, where the risk from tropical cyclones is larger (e.g., Orton et al., 2016).

RSL rise is the primary factor producing nonstationarity in Boston's flood hazard (Figure 5). For example, storm events in 1851 and 1909 each exceeded the modern mean high water datum by ∼1.31 m, approximately 0.16 m less than the January 2018 event. However, RSL rise since then would cause these storm tides to exceed the January 2018 event by 0.1 m, were they to occur today (see Figure 5b). Hence, measured by storm tide (the total rise over annual RSL), the three largest events on record occurred in 1851, 1909, and 1978 (Figures 5 and 6), followed by January 2018. Qualitatively, no obvious temporal trends in skew surge are apparent (Figure 5a), though some clustering of events occurs (such as 1900–1920). Typically, large flood events are correlated with a skew surge of greater than 0.75 m; however, the largest skew surges did not produce the largest total water levels. As we discuss below, the timing of storm events relative to tide forcing plays a determining role.

Most large events (19 out of the top 20) occurred when the predicted tide exceeded mean higher high water, with tides during several events (notably May 1832 and April 1940) occurring close to the highest astronomical tide datum (Figure 6). Fully 92 out of the top 100 events occurred for a predicted tide level greater than the modern mean higher high water of 1.55 m (see supporting information). As described in Wood (1978), many historical extreme water levels in Boston coincided with perigean and proxigean spring tides, again supporting the idea that astronomical tides help control the flood hazard. A high proportion of events occurred around midday or midnight, since large spring tides occur preferentially around this time (first noted by Freeman, 1903, and confirmed here).

Because extratropical cyclones (Nor'Easters) occur multiple times a year, the chance of one occurring during a tide that exceeds mean higher high water and producing elevated water levels is not insignificant. Over an 18.6 year nodal cycle, more than 5% of higher high waters exceed 2 m. Several factors may impact the likelihood that a storm event is phased relative to such a large predicted tide. The time scale (propagation speed and size) of a storm is likely important; for example, the long-acting 1978 extratropical cyclone produced a surge which remained elevated for two consecutive high waters, producing peak water levels on the second high tide (Figure 6a). By contrast, surge in the 1909 and January 2018 events was only elevated over one tidal period (Figure 6a), which by chance was the larger daily high tide. The daily tidal inequality, which sets the relative heights of the daily high tides, varies significantly; for example, virtually no inequality occurred during the 1832 event, whereas about 0.4 m difference occurred between the highest and lowest tide during the 1885 event. Because the diurnal inequality (set by K1 and O1 constituents) is weakest during the peak of the 18.6y nodal cycle in tides (when M2 is maximum; e.g., the situation during the 1830 and 1832 events), the duration of a storm is likely more important during some years than others. Note that the largest tides at Boston occur when lunar declination is at a minimum (e.g., Haigh et al., 2011).

Because large spring tides disproportionately influence Boston flood hazard (Figure 6b), any long-term shift in tide magnitudes will influence extreme water levels. To show the effect of decreasing tide range in the 19th century, we first make tidal predictions based on hourly data (1867–1876 and 1921–2016) and then vary the M2 amplitude annually such that the observed tide range is reproduced (1825–1866 and 1897–1911). Through this approach, we estimate that the predicted high water during the 1851 Minot Ledge event was ∼0.05 m higher when predictions based on mid-19th century tide conditions are considered, versus predictions based on measurements from the year 2000. Similarly, the predicted tidal contribution to the 1832 event would be 0.15 m less if it were to occur today (see ΔTide metric in Figure 6b).

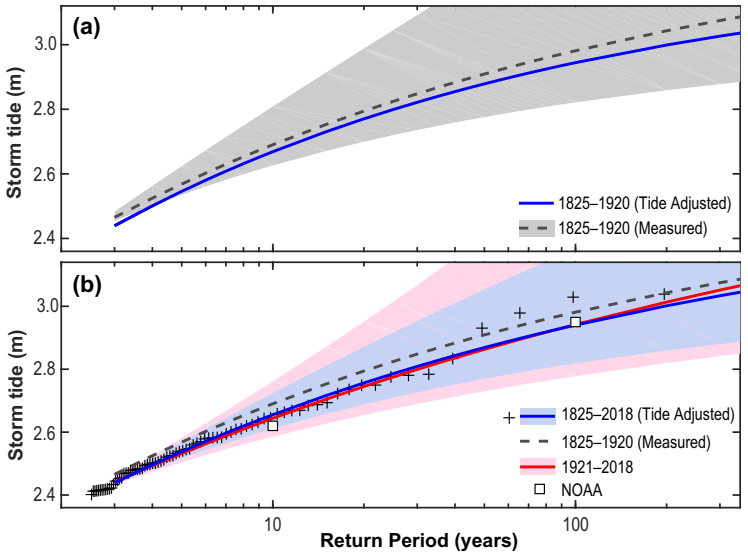

Figure 7. A comparison of the magnitude of storm tides in Boston, as a function of return period. The top plot compares the hazard curve obtained using measured storm tides from 1825 to 1920 (dash-dot line) with a synthetic data set in which the historical storm tides are adjusted by the estimated ΔTide (blue line; see Figure 6). The bottom plot compares the hazard curves found using modern 1921–2018 data (red curve), 1825–1920 records (dashed line), and the entire, adjusted record from 1825 to 2018 (blue line). The fill regions in both panels represent the 1σ confidence interval for the labeled hazard curve. The crosses in Figure 7b denote the unbiased return period estimates for the tide-adjusted 1825–2018 data. The white squares denote NOAA estimates of storm-tide hazard, obtained using a GEV analysis of annual maxima from 1921 to 2017.

We next compare hazard curves obtained using measured storm tides from 1825 to 1920, and a historical storm data set that was adjusted downwards by ΔTide (Figure 6b) to reflect modern tide conditions (Figure 7a). As shown, the adjusted hazard curve was shifted downward by 0.02–0.04 m, indicating that storm-tide risk was likely slightly larger in the early and mid-19th century due to larger tides. The shift in the hazard curve after adjusting for tides (Figure 7a) is small because a large portion of the storm tides, particularly between 1898 and 1919, required a negligible tidal correction (see Figures 4 and 5). These unchanged events may dilute the observed statistical effect of larger mid-19th century tides. The adjustment for evolving tide statistics is however necessary to analyze storm events on a stationary basis (an assumption of the GPD analysis).

After adjusting for 19th century tide trends, we find that the GPD-based hazard curves obtained using the full data set (1825–2018) are indistinguishable from a hazard curve found using only modern data (1921–2018; Figure 7b). The hazard curves also compare well with estimates published by NOAA (square symbols in Figure 7b) and estimates of the unbiased return period (e.g., Makkonen, 2006; see "+" symbols in Figure 7b). The relative shortness of the modern 1921–2018 record produces larger confidence intervals, however. Hence, the primary effect of adding a century of large storm tides to the instrumental record is to reduce the uncertainty bounds around estimates. Unlike New York Harbor (e.g., Talke et al., 2014), we find no evidence of long-term nonstationarity in flood hazard, after accounting for the effects of RSL rise (thru using storm tides) and tidal change. Hence, the increase in storm-tide magnitudes in New York is likely of local or regional cause (either meteorological or hydrodynamic; see e.g., Orton et al., 2015 or Chant et al., 2018).

The effect that a 5.5% decrease in tide range had on hazard curves (Figure 7a) suggests that the 18.6 year nodal cycle also exerts a control on flood risk. The order of magnitude change in tides over a nodal cycle is similar to the 19th century decrease in range; as discussed by Ray and Foster (2016), dominant semidiurnal constituents such as M2 and N2 vary by nearly ±3% over the nodal cycle, while the diurnal K1 constituent varies by ±11%. To better elucidate the effect of such tide variability on storm-tide hazard, we first use harmonic analysis to determine how the 90th percentile of the daily higher high water varies over time (this is the astronomic tide that is exceeded once every 10 days, on average). We restrict our analysis to the 30 October to 30 April time period, primarily because most large events (89 out of top 100) occurred during

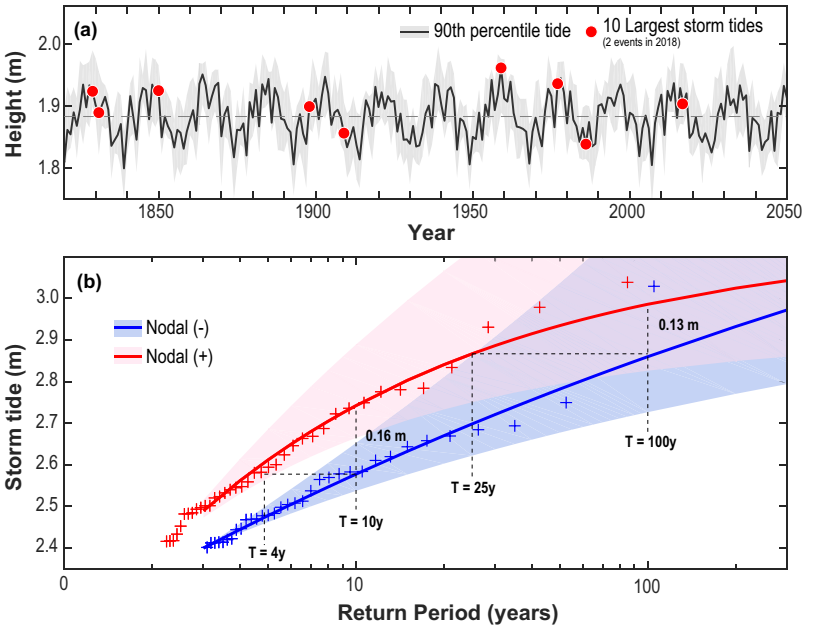

Figure 8. (a) The variation in the magnitude of the 90th percentile of higher water during the storm season, as a function of time. The fill bands denote the ±2.5% percentile bands and provide an indication of how other tide percentiles vary. The years of the top 10 events are shown with red symbols, and the median value of the 90th percentile is shown by a dashed line. (b) A comparison of hazard curves obtained by conditionally sampling the storm tides that occurred during elevated tidal forcing (nodal +) or lesser tidal forcing (nodal −). The nodal + period is defined as a storm season in which the 90th percentile HHW was above the median value of 1.88 m (see Figure 8a), and the nodal (−) period is defined as periods below the median.

this time frame (we chose 30 October to avoid exclusion of events in 1829 and 1991). This sampling approach also prevents biasing statistics by summertime tides (which are larger, on average; see Ray & Foster, 2016) and avoids the introduction of a 4.4 year periodicity that is caused by perigean tides and is often observed in annually calculated high water statistics (e.g., Haigh et al., 2011; see Ray & Foster, 2016 for an explanation).

As shown in Figure 8a, the 90th percentile higher high water during the storm season varies by approximately 0.15 m over the 18.6 year nodal cycle, and is modulated by interannual variability (see also Ray & Foster, 2016). Other tidal statistics such as annual mean high water vary by roughly 0.1 m over a nodal cycle. Because the plurality of historic flood events occurred when the predicted tide exceeded 1.9 m (Figure 6), we hypothesize that the nodal cycle helps control the likelihood of a large event; indeed, a disproportionate share of the largest events (including 1830, 1832, 1851, 1959, 1978, and 2018) occurred near the peak in the nodal cycle for M2 (red circles in Figure 8a; see Figure 5 for absolute heights). To test this hypothesis, we next conditionally sampled our 1825–2018 data set depending on whether it occurred during times of either elevated or suppressed astronomical forcing. A "nodal (+)" and "nodal (–)" period refers to time periods in which the 90th percentile higher high water was greater than, or less than, the median value of ∼1.88 m (Figure 8a).

A GPD analysis of the conditionally sampled data clearly shows that storm-tide hazard is modulated by the 18.6 year nodal cycle (Figure 8b). During the "nodal +" phase, the magnitude of the once-in-10 year and once-in-100 year event probabilities are estimated to be 0.16 and 0.13 m larger than during the "nodal −" phase. Stated differently, a storm-tide magnitude with a 5% chance of occurring during a November to April time period with relatively smaller tides has a more than 10% chance of occurring during a winter with larger tides (Figure 8b). Overall, the magnitude of a 0.01–0.5 probability event is 0.1–0.2 m less during the nodal (−) phase. No overlap occurs in the 1σ confidence bands occurs for a return-period event of 10 years or less, indicating that the difference in hazard is statistically significant. Some overlap in the confidence bands occur for larger return periods, and it is more difficult to statistically distinguish altered risk (Figure 8b). Nonetheless, 8 of the 10 largest storm tides since 1825 occurred during periods of elevated tidal forcing (red circles in Figure 8a), qualitatively confirming our results. Note that Figure 8b is robust to changing the

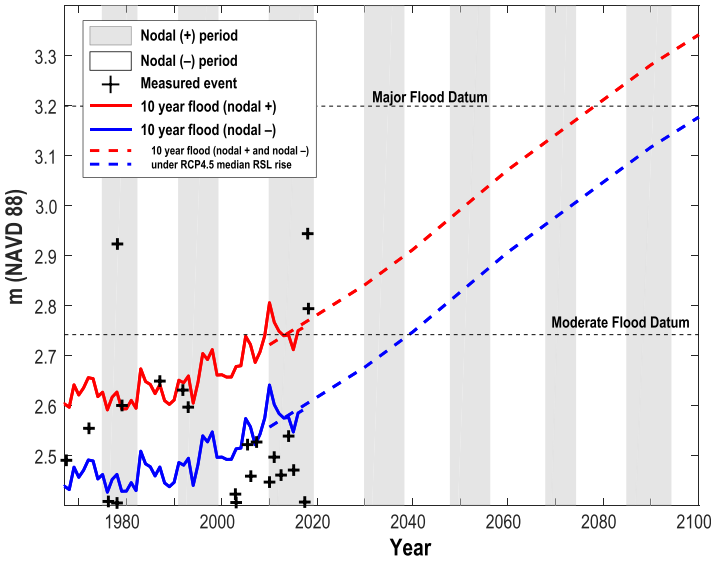

Figure 9. Evolution of the 10 year flood hazard from Figure 8 as RSL in Boston changes, relative to the NAVD-88 datum. The nodal (+) hazard curve, shown in red, is the hazard curve calculated with data from nodal (+) periods (shown with gray banding). The blue nodal (−) curve was obtained from data collected during white banded periods (Figure 8b). Historic high-water marks since 1967 are shown by "+" symbols. Sea level rise from 1967 to 2017 has raised the level of the 10 year event, and is projected to continue rising under the RCP scenario of Kopp et al. (2017), as shown by the dashed line. The appropriate magnitude of the once-in-10 year event will shift from red (gray banded) to blue (white banded periods) on an approximately decadal time scale.

conditional sampling procedure; for example, restricting the "nodal +" and "nodal −" periods to the upper and lower 40% of the nodal cycle (Figure 8a) produces negligible changes in the observed differences in the hazard curves.

The dependency of Boston hazard curves on interannual and decadal fluctuations in tidal properties (Figure 8b) suggests that the time evolution of flood hazard is temporally variable, with contributions caused both by long-term RSL trends and astronomic cycles in tides (e.g., Figure 5 and 8). To demonstrate one possible pathway in which the flood hazard may evolve over the next 80 years, we project the 10 year flood hazard forward in time, using the RCP 4.5 RSL scenario of Kopp et al. (2017). This scenario predicts a median RSL rise of 0.68 m for Boston Harbor between 2000 and 2100, under the assumption that carbon emissions will increase until the mid-21st century, and then slightly decrease. For comparison, the equivalent projection under the business-as-usual RCP 8.5 scenario is 1.25 m. In our approach, we simply add the storm-tide hazard curve (both nodal (+) and nodal (−) scenarios) to RSL, without consideration of nonlinear feedbacks, nonstationarity in tides, or nonstationarity in storm magnitudes. Since the rate of tide change appears to have decreased since the 1980s (Ray & Foster, 2016) and no evidence of nonstationarity in storm magnitudes is found (Figure 7b), this approach is a good first estimate. Error bounds for the 10 year flood risk are found in Figure 8b, and likelihood estimates for the RCP 4.5 sea level rise scenario are found in Kopp et al. (2017).

Projections show that RSL rise will greatly increase the probability of both moderate and major flooding, such that a major flood may have a one-in-10 chance of occurring by the end of the century in any given year (Figure 9). A distinct variability in hazard occurs during the 18.6 year nodal cycle, however. During the 2020s, tidal forcing (nodal (−) phase) will be relatively smaller during the storm season and will tend to reduce flood hazard. The reduced contribution of tides to the total water level may be partially offset by continued RSL rise, resulting in an approximate stationarity in overall flood risk. By contrast, during the 2030s, the combination of a nodal (+) phase in tides plus RSL rise may abruptly increase flood risk. Such a pattern is projected to repeat itself during the 21st century on roughly a decadal time-line (Figure 9). The relative importance of tidal modulations becomes smaller and smaller through the remainder of the 21st century, as RSL rise rates increase.

Our results confirm insights from global surveys of tide-gauge data and satellite altimetry, which previously showed that the nodal (18.6 year) and perigean (8.85 year) modulation of tides affects the 99.9th % exceedance value of hourly data (roughly equivalent to an event that occurs 8–9 times a year; see Elliot, 2010; Haigh et al., 2011; Woodworth & Blackman, 2004) and modulates the location parameter in a nonstationary hazard assessment (e.g., Menendez & Woodworth, 2010). Similarly, other studies pointed out the controlling factor that tide maxima exert on monthly or annual extremes globally, and the sensitivity of flooding frequency to sea-level rise (e.g., Merrifield et al., 2013; Rueda et al., 2017). These studies all evaluated satellite data since the early 1990s or tide-gauge records of $<$50 years in length, both of which are relatively short periods compared to the nodal cycle. Our results build on these studies by evaluating a much longer data set, which increases the likelihood that a representative sample of large storm tides was obtained over multiple nodal cycles. This enables empirical analysis of more impactful, smaller probability storms such as the 10 year and 100 year events. Nonetheless, our approach assumes quasi-stationarity between different phases of the nodal cycle, and an approach that allows for a year-by-year fluctuation in risk might increase the predictive skill of our analysis (see e.g., Menendez & Woodworth, 2010).

Combined with the results of previous studies (Menendez & Woodworth, 2010; Woodworth & Blackman, 2004), our case study of Boston suggests that the superposition of tidal forcing and sea-level rise likely produces a significant modulation in risk in other regions of the northwest Atlantic Ocean and anywhere in which tidal forcing is relatively large compared to the meteorological surge (see also Rueda et al., 2017). In

particular, since the hazard curve (Figure 7) is relatively flat with respect to return period, a modest change in either RSL or tide amplitude produces a relatively large shift in return period. Over the ~200 year record, 0.28 m of RSL rise decreased the once-in-100 year extreme water level in the 1820s to a probability of ~0.1 (a once-in-10 year event). This flat hazard curve, which is typical for regions with large tide ranges and primarily extratropical storms, also explains why changes to tides (whether over monthly, annual, nodal, or secular time scales) exert an outsized influence on the flood hazard in Boston Harbor.

The implications of RSL rise on flood risk are already beginning to be observed. Relative to a fixed datum, six of the top 20 known peak water levels since 1723 occurred since 2005, and 8 of the top 25 (see supporting information). Similarly, 1/3 of the top 100 water levels (33 events) since 1825 occurred within 2005–2018, far out of proportion with historical norms (see supporting information data sets). More than half (55%) of the top 100 events relative to a fixed datum occurred over 1968–2018. Elevated water levels that were once rare are becoming increasingly common as RSL increases and the rate of rise accelerates.

4. Conclusions

We recovered water-level measurements made in Boston Harbor since 1825 and combined them with existing records from the NOAA tide gauge to obtain a nearly 200 year long history of RSL change, tides and extreme events. Direct and indirect analysis methods and archival records were used to assess historical measurement precision, identify occasional periods with larger uncertainty, and estimate possible datum bias. Moreover, multiple lines of evidence were used to transfer the datum from the historical to the modern gauge location, increasing confidence. A slight ($<$0.03 m) bias was discovered in the early and mid-20th century Boston record due primarily to early data being referenced to unstable benchmarks. The extended record is the longest of its type outside of northwestern Europe.

RSL rose in Boston Harbor by ~0.28 m since the 1820s, including a linear contribution of ~0.5 mm/yr from ongoing land motion caused by GIA. Over the entire record, RSL in Boston accelerated at $\sim 0.023 \pm 0.09$ mm/yr^2, which is broadly consistent with estimates of global mean sea level rise acceleration generated from compilations of tide-gauge records (e.g., Dangendorf et al., 2017; Hay et al., 2015; Jevrejeva et al., 2014). Since the early 20th century, the rate of RSL rise has increased. After removing the estimated contribution from GIA, the extended Boston RSL record agrees well with decadal-scales trends measured in New York City. The small annual differences between these locations occur due to GIA uncertainty, measurement uncertainty, and (at least recently) differences in dynamical ocean processes.

Identifying the onset of modern sea-level rise remains an area of active research (e.g., Gehrels & Woodworth, 2013). Archival data recovery efforts such as this contribution are making clear that under-utilized records from the 19th and early 20th century exist and can address analysis limitations caused by the limited length and (lack of) spatial distribution of instrumental data sets (e.g., Hogarth, 2014; Marcos et al., 2011; Talke & Jay, 2013, 2017; Watson, 2011; Wöeppelman et al., 2014; Woodworth & Blackman, 2002). Our archival research approach builds on previous efforts by (a) investigating nonstandard sources for data, including the personal papers of local engineers; (b) digitizing and evaluating the gauge checks associated with the records; (c) evaluating correspondence letters for gauge quality information and metadata; and (d); painstakingly aggregating sources of error and estimating error (Table 1; supplement). The labor-intensive approach has yielded insights into the data quality of both historic and modern records; for example, we have corrected the seasonal cycle of New York data from 1856 to 1861 and fixed a slight bias in the early to mid-20th century Boston record. These corrections only affect the details, but not the general trends, of sea level rise. Nonetheless, since Burgette et al. (2009) observed similar order-of-magnitude datum issues at two long-term gauges in the Pacific Northwest (Charleston and Astoria, OR), we suggest that a general reanalysis of early records may be desirable. A better assessment of uncertainty (e.g., Table 1) may help improve upon statistical techniques which aggregate historical sea-level data into a global trend (cf. Hay et al., 2015).

Archival records show that tidal range in Boston Harbor decreased by 5.5% since the early 19th century, but increased slightly since 1921. Because large tides in Boston Harbor contribute to the frequency and magnitude of flooding, characterizing the reasons for nonstationarity in tides has important implications for better assessing flood hazard. Our analysis suggests that the primary causes of long-term trends in tidal constituents is the widespread land reclamation and channel deepening that occurred throughout Boston harbor in

the 19th century and 20th centuries. Regional-scale changes in tidal properties in the Gulf of Maine also likely contribute (Ray, 2006).

We used the extended data set of water-level measurements to estimate the height and causes of extreme high-water levels over the past ~300 years, and construct a nearly continuous record of large storm tides since 1825. These records confirm that the flood hazard in Boston for return periods less than 300 years is primarily set by extratropical events (Nor'Easters) which generally occur from November to April. Moreover, the extended record suggest that flood hazard is strongly influenced by variations in tidal forcing over the 18.6 year tide cycle, such that the magnitudes of storm-tide events with return period of 2–100 years are reduced by 0.1–0.2 m during periods of relatively smaller tides. Over the past century, RSL rise reduced the return interval of any given extreme water level, such that approximately 1/3 of the top 100 measured events over the past 200 years have occurred in the last 12, including two recent events in 2018 that are ranked first and third, respectively, relative to a fixed datum. The recent flooding in 2018 and most other large events occurred near the peak of the nodal cycle and during a period of large spring tides.

The frequency and magnitude of future coastal flooding in Boston will be controlled by RSL rise that is anticipated to accelerate further. Variations in tidal forcing, from daily cycles to long-term trends (see Ray & Foster, 2016), will also contribute to a time-variable flood hazard. Return-period probabilities will be approximately stationary during the 2020s because RSL rise and a nodal(−) phase in tidal range counteract one another. In the 2030s RSL rise and a nodal(+) phase will combine to abruptly elevate the risk of coastal flooding. These considerations suggest that planning for coastal infrastructure, flood defense, and bathymetric modifications should take into account both the timing and magnitude of long-term fluctuations and trends in tidal forcing, along with projections of RSL rise.

Acknowledgments
Student digitizers at Portland State University and Tufts University are thanked for their tireless efforts to input historical tide data into spreadsheets. Peter Hogarth is thanked for helpful discussions regarding the Boston datum, and David Jay for helpful discussions on tides. Mark Merrifield and an anonymous reviewer are thanked for their helpful comments, which greatly improved the text. S. A. Talke was funded by the US Army Corps of Engineers (award W1927N-14-2-0015) and the NSF CAREER award 1455350, and both S. A. Talke and A. C. Kemp were funded by the MA Sea Grant. Niamh Cahill performed the change point analysis on the relative sea level time series. Archivists at the National Archives in College Park, MD are thanked (especially Eugene Morris), as well as archivists at MIT (especially Nora Murphy) and Harvard University for their assistance in identifying and using the materials of the engineers Laommi Baldwin Jr. and John R. Freeman. As a historical note, we recognize J. R. Freeman for his intrepid search of leveling surveys and water-level observations from the 19th century, which might otherwise be lost. His records show, for example, that he partially found and helped preserve the Baldwin records from the 1820s and 1830s. Moreover, he was one of the first to recognize that Boston and New York Cty were experiencing subsidence and may have been one of the first to recognize the onset of modern sea level rise (see supporting information). Additional information about the archival data, the historical datum, and data processing are included in the supporting information and the relative sea level and storm-tide record used in this manuscript are included as supporting information.

References

Agnew, D. A. (1986). Detailed analysis of tide gauge history: A case analysis. *Marine Geodesy*, *10*(3–4), 231–255.
Arns, A., Dangendorf, S., Jensen, J., Bender, J., Talke, S. A., & Pattiaratchi, C. (2017). Sea-level rise induced amplification of coastal protection design heights. *Nature: Scientific Reports*, *7*, 40171. https://doi.org/10.1038/srep40171
Baldwin archives. Harvard Business School. Retrieved from http://oasis.lib.harvard.edu/oasis/deliver/~bak00153
Baldwin, G. (1864). *Report of the Joint Committee of 1860 upon The Proposed Canal to unite Barnstable and Buzzard's Bays, 1864* (Public Doc. 41, pp. 125–129). Boston, MA: Wright & Potter, State Printers.
Bearss, E. C. (1984). *Charlestown Navy Yard, 1800–1842* (2 Vols.). Denver, CO: National Park Service.
Bromirski, P. D., Flick, R. E., & Cayan, D. R. (2003). Storminess variability along the California coast: 1858–2000. *Journal of Climate*, *16*(6), 982–993.
Burgette, R. J., Weldon, R. J. II., & Schmidt, D. A. (2009). Interseismic uplift rates for western Oregon and along-strike variation in locking on the Cascadia subduction zone. *Journal of Geophysical Research*, *114*, B01408. https://doi.org/10.1029/2008JB005679
Chant, R. J., Sommerfeld, C. K., & Talke, S. A. (2018). Impact of channel deepening on tidal and gravitational circulation in a highly engineered estuarine basin. *Estuaries & Coasts*. https://doi.org/10.1007/s12237-018-0379-6
Chernetsky, A. S., Schuttelaars, H. M., & Talke, S. A. (2010). The effect of tidal asymmetry and temporal settling lag on sediment trapping in tidal estuaries. *Ocean Dynamics*, *60*, 1219–1241. https://doi.org/10.1007/s10236-010-0329-8
Church, J. A., & White, N. J. (2011). Sea-level rise from the late 19th to the early 21st century. *Surveys in Geophysics*, *32*, 585–602. https://doi.org/10.1007/s10712-011-9119-1
Dangendorf, S., Marcos, M., Wöppelmann, G., Conrad, C. P., Frederikse, T., & Riva, R. (2017). Reassessment of 20th century global mean sea level rise. *Proceedings of the National Academy of Sciences of the United States of America*, *114*, 5946–5951.
Davis, J. L., & Mitrovica, J. X. (1996). Glacial isostatic adjustment and the anomalous tide gauge record of eastern North America. *Nature*, *379*, 331–333. https://doi.org/10.1038/379331a0
Davis, J. L., & Vinogradova, N. T. (2017). Causes of accelerating sea level on the East Coast of North America. *Geophysical Research Letters*, *44*, 5133–5141. https://doi.org/10.1002/2017GL072845
Dronkers, J. J. (1964). *Tidal computations in rivers and coastal waters* (pp. 219–304). North-Holland, Amsterdam: Wiley Interscience.
Eliot, M. (2010). Influence of interannual tidal modulation on coastal flooding along the Western Australian coast. *Journal of Geophysical Research*, *115*, C11013. https://doi.org/10.1029/2010JC006306
Engelhart, S. E., & Horton, B. P. (2012). Holocene sea level database for the Atlantic coast of the United States. *Quaternary Science Reviews*, *54*, 12–25.
Familkhalili, R., & Talke, S. A. (2016). The effect of channel deepening on storm surge: A case study of Wilmington, NC. *Geophysical Research Letters*, *43*, 9138–9147. https://doi.org/10.1002/2016GL069494
Foreman, M. G. G. (1977). *Manual for tidal currents analysis and prediction* (Pac. Mar. Sci. Rep. 77-10, 101 p.). Sidney, BC: Institute of Ocean Sciences.
Frederikse, T., Simon, K., Katsman, C. A., & Riva, R. (2017). The sea-level budget along the Northwest Atlantic coast: GIA, mass changes, and large-scale ocean dynamics. *Journal of Geophysical Research: Oceans*, *122*, 5486–5501. https://doi.org/10.1002/2017JC012699
Freeman, J. R. (1903). *Committee on Charles River Dam; Report of the Committee on Charles River Dam, appointed under resolves of 1901, chapter 105, to consider the advisability and feasibility of building a dam across the Charles River at or near Craigie bridge. Appendix 20*. Boston, MA: Wright and Potter Printing Co., State Printers.
Freeman, J. R. (1904). *Report on the improvement of the Upper Mystic River and Alewife Brook*. Boston, MA: Wright & Potter Printing Co., State Printers.

Friedrichs, C. T., & Aubrey, D. G. (1994). Tidal propagation in strongly convergent channels. *Journal of Geophysical Research*, *99*, 3321–3336. https://doi.org/10.1029/93JC03219

Gehrels, W. R., & Woodworth, P. (2013). When did modern rates of sea-level rise start?. *Global and Planetary Change*, *100*, 263–277.

Goddard, P. B., Yin, J., Griffies, S., & Zhang, S. (2015). An extreme event of sea-level rise along the Northeast coast of North America in 2009–2010. *Nature Communications*, *6*, 6346. https://doi.org/10.1038/ncomms7346

Godin, G. (1991). Compact approximations to the bottom friction term, for the study of tides propagating in channels. *Continental Shelf Research*, *11*(7), 579–589.

Haigh, I. D., Elliot, M., & Pattiaratchi, C. (2011). Global influences of the 18.61 year nodal cycle and 8.85 year cycle of lunar perigee on high tidal levels. *Journal of Geophysical Research*, *116*, C06025. https://doi.org/10.1029/2010JC006645

Haigh, I. D., Wahl, T., Rohling, E. J., Price, R. M., Pattiaratchi, C. B., Calafat, F. M., & Dangendorf, S. (2014). Timescales for detecting a significant acceleration in sea level rise. *Nature Communications*, *5*, 3635. https://doi.org/10.1038/ncomms4635

Hay, C. C., Morrow, E., Kopp, R. E., & Mitrovica, J. X. (2015). Probabalistic reanalysis of twentieth-century sea-level rise. *Nature*, *517*, 481–484. https://doi.org/10.1038/nature14093

Hogarth, P. (2014). Preliminary analysis of acceleration of sea level rise through the 20th century using extended tide gauge data sets. *Journal of Geophysical Research*, *119*, 7645–7659. https://doi.org/10.1002/2014JC009976

Hudson, A. S., Talke, S. A., Branch, R., Chickadel, C., Farquharson, G., & Jessup, A. (2017). Remote measurements of tides and river slope using airborne lidar instrument. *Journal of Atmospheric and Oceanic Technology*, *34*(4), 897–904. https://doi.org/10.1175/JTECH-D-16-0197.1

Jevrejeva, S., Moore, J. C., Grinsted, A., Matthews, A. P., & Spada, G. (2014). Trends and acceleration in global and regional sea levels since 1807. *Global Planet Change*, *113*, 11–22.

Jevrejeva, S., Moore, J. C., Grinsted, A., & Woodworth, P. L. (2008). Recent global sea level acceleration started over 200 years ago? *Geophysical Research Letters*, *35*, L08715. https://doi.org/10.1029/2008GL033611

Karegar, M. A., Dixon, T. H., & Engelhart, S. E. (2016). Subsidence along the Atlantic Coast of North America: Insights from GPS and late Holocene relative sea level data. *Geophysical Research Letters*, *43*, 3126–3133. https://doi.org/10.1002/2016GL068015

Kemp, A. C., & Horton, B. P. (2013). Contribution of relative sea-level rise to historical hurricane flooding in New York City. *Journal of Quaternary Science*, *28*, 537–541.

Kemp, A. C., Horton, B. P., Vane, C. H., Corbett, D. R., Bernhardt, C. E., Engelhart, S. E., et al. (2013). Sea-level change during the last 2500 years in New Jersey, USA. *Quaternary Science Reviews*, *81*, 90–104.

Kopp, R. E. (2013). Does the mid-Atlantic United States sea-level acceleration hot spot reflect ocean dynamic variability?. *Geophysical Research Letters*, *40*, 3981–3985. https://doi.org/10.1002/grl.50781

Kopp, R. E., DeConto, R. M., Bader, D. A., Horton, R. M., Hay, C. C., Kulp, S., et al. (2017). Implications of Antarctic ice-cliff collapse and ice-shelf hydrofracturing mechanisms for sea-level projections. *Earth's Future*, *5*, 1217–1233.

Kotz, S., & Nadarajah, S. (2000). *Extreme value distributions: Theory and applications*. London, UK: Imperial College Press.

Kukulka, T., & Jay, D. A. (2003). Impacts of Columbia River discharges on salmonid habitat: 1. A nonstationary fluvial tidal model. *Journal of Geophysical Research*, *108*(C9), 3293. https://doi.org/10.1029/2002JC001382

Landerer, F. W., Jungclaus, J. H., & Marotzke, J. (2007). Regional dynamic and steric sea level change in response to the IPCC-A1B scenario. *Journal of Physical Oceanography*, *37*(2), 296–312. https://doi.org/10.1175/JPO3013.1

Leffler, K. E., & Jay, D. A. (2009). Enhancing tidal harmonic analysis: Robust (hybrid L1/L2) solutions. *Continental Shelf Research*, *29*, 78–88.

Ludlam, D. M. (1963). *Early American Hurricanes, 1492–1870* (198 p.). Boston, MA: American Meteorological Society.

Makkonen, L. (2006). Plotting positions in extreme value analysis. *Journal of Applied Meteorology and Climatology*, *45*, 334–340.

Marcos, M., Puyol, B., Wöppelmann, G., Herrero, C., & GarCía-Fernández, M. J. (2011). The long sea level record at Cadiz (southern Spain) from 1880 to 2009. *Journal of Geophysical Research*, *116*, C12003. https://doi.org/10.1029/2011JC007558

Maul, G. A., & Martin, D. M. (1993). Sea level rise at Key West Florida, 1846–1992: America's longest instrument record? *Geophysical Research Letters*, *20*(18), 1955–1958.

Menéndez, M., & Woodworth, P. L. (2010). Changes in extreme high water levels based on a quasi-global tide-gauge dataset. *Journal of Geophysical Research*, *115*, C10011. https://doi.org/10.1029/2009JC005997

Merrifield, M. A., Genz, A. S., Kontoes, C. P., & Marra, J. J. (2013). Annual maximum water levels from tide gauges: Contributing factors and geographic patterns. *Journal of Geophysical Research*, *118*, 2535–2546. https://doi.org/10.1002/jgrc.20173

Moftakhari, H. R., Jay, D. A., & Talke, S. A. (2016). Estimating river discharge using multiple-tide gages distributed along a channel. *Journal of Geophysical Research: Oceans*, *121*, 2078–2097. https://doi.org/10.1002/2015JC010983

Müller, M. (2011). Rapid change in semi-diurnal tides in the North Atlantic since 1980. *Geophysical Research Letters*, *38*, L11602. https://doi.org/10.1029/2011GL047312

Parker, B. B. (1991). The relative importance of the various nonlinear mechanisms in a wide range of tidal interactions. In B. B. Parker (Ed.), *Progress in tidal hydrodynamics* (pp. 237–268). New York, NY: John Wiley.

Pawlowicz, R., Beardsley, B., & Lentz, S. (2002). Classical tidal harmonics analysis including error estimates in MATLAB using T-TIDE. *Computational Geosciences*, *28*, 929–937.

Peltier, W. R. (2004). Global glacial isostasy and the surface of the ice-age Earth: The ICE-5G (VM2) model and GRACE. *Annual Review of Earth and Planetary Sciences*, *32*, 111–149.

Perley, S. (1891). *Historic storms of New England*. Salem, MA: The Salem Press Publishing and Printing Co.

Piecuch, C. G., & Ponte, R. M. (2015). Inverted barometer contributions to recent sea level changes along the northeast coast of North America. *Geophysical Research Letters*, *42*, 5918–5925. https://doi.org/10.1002/2015GL064580

Public Works Department (PWD) (1922). *Annual report of the public works department for the year 1921* (117 p.). Boston, MA: City of Boston Printing Department.

Orton, P. M., Hall, T. M., Talke, S. A., Georgas, N., Blumberg, A. F., & Vinogradov, S. (2016). A validated tropical-extratropical flood hazard assessment for New York harbor. *Journal of Geophysical Research: Oceans*, *121*, 8904–8929. https://doi.org/10.1002/2016JC011679

Orton, P. M., Talke, S. A., Jay, D. A., Yin, L., Blumberg, A. F., Georgas, N., et al. (2015). Channel Shallowing as Mitigation of Coastal Flooding. *Journal of Marine Science and Engineering*, *3*(3), 654–673. https://doi.org/10.3390/jmse3030654

Rahmstorf, S., & Vermeer, M. (2011). Discussion of: Houston, J.R. and Dean, R.G., 2011. Sea-Level Acceleration Based on U.S. Tide Gauges and Extensions of Previous Global-Gauge Analyses. *Journal of Coastal Research*, *27*(3), 409–417.

Ray, R. D. (2006). Secular changes of the M2 tide in the Gulf of Maine. *Continental Shelf Research*, *26*, 422– 427.

Ray, R. D., & Foster, G. (2016). Future nuisance flooding at Boston caused by astronomical tides alone. *Earth's Future*, *4*, 578–587. https://doi.org/10.1002/2016EF000423

Rueda, A., Vitousek, S., Camus, P., Tomás, A., Espejo, A., Losada, I. J., et al. (2017). A global classification of coastal flood hazard climates associated with large-scale oceanographic forcing. *Scientific Reports*, *7*, 5038. https://doi.org/10.1038/s41598-017-05090-w

Sallenger, A. H., Doran, K. S., & Howd, P. A. (2012). Hotspot of accelerated sea-level rise on the Atlantic coast of North America. *Nature Climate Change*, *2*, 884–888. https://doi.org/10.1038/nclimate1597

Schureman, P. (1928). *Tides and currents in Boston Harbor* (Special Publ. 142, 144 p.). Washington DC: US Coast and Geodetic Survey, United States Government Printing Office.

Seasholes, N. S. (2003). *Gaining ground: A history of landmaking in Boston*. Cambridge, MA: MIT Press.

Smith, F. H. Jr. (1917). *Storms and shipwrecks in Boston Bay and the record of the life savers of Hull* (Vol. II). Boston, MA: The Bostonian Society T.R. Marvin & Son Printers.

Talke, S. A., & Jay, D. A. (2013). Nineteenth century North American and Pacific tide data: Lost or just forgotten? *Journal of Coastal Research*, *29*(6), 118–127.

Talke, S. A., & Jay, D. A. (2017). *Archival water-level measurements: Recovering historical data to help design for the future* (CWTS Rep. 2017-02). US Army Corps of Engineers. Retrieved from http://corpsclimate.us/docs/Recovering_Historical_Data_AUGUST-2017.pdf

Talke, S. A., Orton, P., & Jay, D. A. (2014). Increasing storm tides in New York Harbor, 1844–2013. *Geophysical Research Letters*, *41*, 3149–3155. https://doi.org/10.1002/2014GL059574

United States Congress (2014). *H.R. 3080 (113th): Water Resources Reform and Development Act of 2014*.

United States House of Representatives (USHR) (1830). *Executive Documents of the House of Representatives at the second session of the Twenty-First Congress, begun and Held at the City of Washington, Dec. 6 1830, And in the Fifty-fifth year of the Independence of the United States* (Document 2, Part C, pp. 206–207).

Wang, J., Yi, S., Mengya, L., Wang, L., & Song, C. (2018). Effects of sea level rise, land subsidence, bathymetric change and typhoon tracks on storm flooding in the coastal areas of Shanghai. *Science of the Total Environment*, *621* (2018), 228–234.

Watson, P. J. (2011). Is there evidence yet of acceleration in mean sea level rise around mainland Australia?. *Journal of Coastal Research*, *27*(2), 368–377.

Williams, J., Horsburgh, K. J., Williams, J. A., & Proctor, R. N. F. (2016). Tide and skew surge independence: New insights for flood risk. *Geophysical Research Letters*, *43*, 6410–6417. https://doi.org/10.1002/2016GL069522

Wood, F. (1978). *The strategic role of perigean spring tides in nautical history and North American coastal flooding, 1635–1976* (529 p.). Rockville, MD: U.S. Department of Commerce, National Oceanic and Atmospheric Administration.

Woodworth, P. L. (2010). A survey of recent changes to the main components of the ocean tide. *Continental Shelf Research*, *30*(15), 1680–1691.

Woodworth, P. L., & Blackman, D. L. (2002). Changes in extreme high waters at Liverpool since 1768. *International Journal of Climatology*, *22*, 697–714. https://doi.org/10.1002/joc.761

Woodworth, P. L., & Blackman, D. L. (2004). Evidence for systematic changes in extreme high waters since the mid-1970s. *Journal of Climate*, *17*(6), 1190–1197. https://doi.org/10.1175/1520-0442(2004)017

Woodworth, P. L., White, N. J., Jevrejeva, S., Holgate, S. J., Church, J. A., & Gehrels, W. R. (2009). Evidence for the accelerations of sea level on multi-decade and century timescales. *International Journal of Climatology*, *29*(6), 777–789.

Wöppelmann, G., Marcos, M., Coulomb, A., Martín Míguez, B., Bonnetain, P., & Boucher, C. (2014). Rescue of the historical sea level record of Marseille (France) from 1885 to 1988 and its extension back to 1849–1851. *Journal of Geodesy*, *88*, 869–885. https://doi.org/10.1007/s00190-014-0728-6

Zaron, E. D., & Jay, D. A. (2014). An analysis of secular change in tides at open-ocean sites in the Pacific. *Journal of Physical Oceanography*, *44*(7), 1704–1726.

Zervas, C., Gill, S., & Sweet, W. (2013). *Estimating vertical land motion from long-term tide gauge records* (Tech. Rep. NOS CO-OPS 065, 20 p.). Silver Spring, MD: National Oceanic and Atmospheric Administration.